Spontaneous Emission Spectrum in Double Quantum Dot Devices

Toshimasa Fujisawa[1;2], Tjerk H. Oosterkamp[1], Wilfred G. van der Wiel[1], Benno W. Broer[1], Ramón Aguado[1], Seigo Tarucha[2;3] and Leo P. Kouwenhoven[1].
[1]Department of Applied Physics and DIMES, Delft University of Technology, P.O. Box 5046, 2600 GA Delft, The Netherlands.
[2]NTT Basic Research Laboratories, 3-1, Morinosato-Wakamiya, Atsugi, Kanagawa, 243-0198, Japan.
[3]Department of Physics, University of Tokyo, 7-3-1 Hongo, Bunkyo-ku, Tokyo 113-0033, Japan.
(submitted to Science on July 23, 1998, resubmitted on Sept. 30, 1998, accepted for publication in Science.)

A double quantum dot device is a tunable two-level system for electronic energy states. A dc electron current directly measures the rates for elastic and inelastic transitions between the two levels. For inelastic transitions energy is exchanged with bosonic degrees of freedom in the environment. The inelastic transition rates are well described by the Einstein coefficients, relating absorption with stimulated and spontaneous emission. The most effectively coupled bosons in the specific environment of our semiconductor device are acoustic phonons. The experiments demonstrate the importance of vacuum fluctuations in the environment for quantum dot devices and potential design constraints for their use for prepairing long-lived quantum states.

Electronic quantum devices allow the quantum mechanical properties of electrons confined to small regions in a solid to be explored. Existing devices include semiconductor resonant tunneling diodes (1) (based on quantum mechanical confinement), superconducting Josephson junction circuits (2) (based on macroscopic phase coherence), metallic single electron transistors (3) (based on quantization of charge), and molecular electronic devices (4). The principle of operation in circuits of these devices is based on controlling energy states, for instance, by means of an external (gate) voltage. Thermal energy is always a source for unwanted transitions and errors. Even at zero temperature, however, vacuum fluctuations in the environment can give rise to transitions between states of non-equal energy by spontaneous emission of an energy quantum. Such inelastic transitions cause errors in many proposed schemes for quantum circuits. We have studied inelastic transitions in a fully-controllable, two-level quantum system realized in a double quantum dot device. We can relate the transition rates involving emission to absorption rates by the Einstein coefficients over the full energy and temperature range we studied. At our lowest temperature (23 mK), we directly measured the energy-dependent rate for spontaneous emission. In our specific semiconductor device, this energy is emitted into the environment formed by acoustic phonons.

Our double quantum dot (Fig. 1A) is fabricated in the two-dimensional electron gas (2DEG) of an AlGaAs/GaAs semiconductor heterostructure (5). The source and drain are large 2DEG regions that serve as leads for contacting current and voltage wires. The two dots, L and R, are separated from each other and from the leads by potential barriers induced by negative voltages applied to the three metallic gates. Tunneling between the different regions is sufficiently strong to detect current but weak enough that the number of electrons in each dot is a well-defined integer. The energy states in such fully confined regions are discrete, 0D-states; resembling discrete atomic states (6, 7). The discrete energies include contributions from single-electron charging energies, arising from Coulomb interactions, and from quantum-mechanical confinement. The lowest energy state for one additional electron in the left dot is labeled in Fig. 1, B to D, as E_L and similarly E_R for the right dot. Figure 1C illustrates the resonance condition, $E_L = E_R$, in which case an electron can tunnel elastically from an occupied state in the source via E_L and E_R to an empty state in the drain. Such tunneling sequences of single electrons are regulated by the Coulomb charging energies (3, 7). When the two states are not aligned, $E_L \neq E_R$, only inelastic transitions are allowed for which some energy needs to be exchanged with the environment. A measured off-resonance current, therefore, directly provides information about the coupling between electrons on the dots to degrees of freedom in the environment. The inelastic rates can be analyzed with well-developed methods in quantum optics (8, 9).

Figure 1E shows a typical current spectrum versus $\varepsilon \equiv E_L - E_R$ at our lowest lattice temperature T = 23 mK (10). The gate voltages V_{GR} and V_{GL} are swept simultaneously such that the respective energies are like in Fig. 1, B to D; that is, $\varepsilon = 0$ occurs in the middle between the Fermi energies of source and drain, μ_S and μ_D, and $|\varepsilon| = eV_{SD}$ (its maximum) corresponds to having the states E_L and E_R aligned to one of the Fermi energies. To analyze the large asymmetry, we decompose the total current $I_{tot}(\varepsilon) = I_{el}(\varepsilon) + I_{inel}(\varepsilon > 0)$ into a symmetric part $I_{el}(\varepsilon) = I_{el}(-\varepsilon)$ (dashed curve) and the remaining asymmetric part $I_{inel}(\varepsilon > 0)$ (dotted-dashed curve). At T = 0, $I_{el}(\varepsilon)$ is due to elastic tunneling and

has a Lorentzian line shape $I_{el}(\varepsilon) = I_{el;max}w^2/(w^2 + \varepsilon^2)$ (11). The full-width at half-maximum (FWHM), 2w; can be tuned by the central gate voltage V_{GC} roughly from 4 to 20 μeV. From measurements of $I_{el}(\varepsilon)$ at positive and negative V_{SD}, it is possible to extract values for the tunnel couplings γ_L, γ_R and T_c (11, 12).

The remaining current, $I_{inel}(\varepsilon > 0)$; which is non-zero only for $\varepsilon > 0$, is due to inelastic tunneling. In Fig. 1E, I_{inel} is non-zero over an energy range of »100 μeV, despite the thermal energy kT (23 mK) = 2 μeV being much smaller (k is Boltzmann's contant). (The irregular fine structure is discussed below.) In general, we find that I_{inel} vanishes when one of the levels, E_L or E_R, crosses one of the two Fermi energies. In the specific case of Fig. 1E, E_L and E_R cross the Fermi energies simultaneously, implying that I_{inel} is cut off at $\varepsilon = eV_{SD}$. Below this cut off, the value of I_{inel} was not influenced by the value of V_{SD} (13). For T = 0, we can write the condition for a non-zero inelastic current as $\mu_S > E_L > E_R > \mu_D = \mu_S - eV_{SD}$. The amount of inelastic current depends on the transition rates as: $I_{inel}(\varepsilon) = e(\gamma_L^{-1} + \gamma_i^{-1}(\varepsilon) + \gamma_R^{-1})^{-1}$. When the inelastic rate $\gamma_i(\varepsilon)$ from E_L to E_R is much smaller than the rates through the outer barriers, then $I_{inel}(\varepsilon) = e\gamma_i(\varepsilon)$:

The effect of a non-zero temperature on the current is shown in Fig. 2A. A higher temperature T, enhances I_{tot} on both the emission ($\varepsilon > 0$) and the absorption ($\varepsilon < 0$) side. The absorption spectrum shows an exponential temperature dependence, $e^{\varepsilon/kT}$ (dashed lines) for absolute energies larger than the elastic current measured at 23 mK, that is $|\varepsilon| > w$:

To analyze the temperature dependence, we assume boson statistics for the degrees of freedom in the environment. The average occupation number $\langle n\rangle$ of environmental modes at energy ε is given by the Bose-Einstein distribution function: $\langle n\rangle = 1/(e^{\varepsilon/kT} - 1)$. The rates for absorption, W_a, and emission, W_e, can be expressed very generally by $W_a = B_a\rho$ and $W_e = A + B_e\rho$, where the Einstein coefficients stand for spontaneous emission (A), stimulated emission (B_e) and absorption (B_a), and ρ is the energy density (8). From the Einstein relations, $B_a = B_e = A\langle n\rangle/\rho$ (8), we obtain:

$$\gamma_i(\varepsilon < 0) = W_a(\varepsilon) = \langle n\rangle A(-\varepsilon) \qquad (1)$$
$$\gamma_i(\varepsilon > 0) = W_e(\varepsilon) = (\langle n\rangle + 1)A(\varepsilon)$$

To test whether the inelastic current follows emission and absorption statistics, we calculate the full current spectrum from Eq. 1. First, we obtain the spontaneous emission rate from $A(\varepsilon) = I_{inel}(\varepsilon > 0, T = 23\ \text{mK})/e$: The trace at 23 mK is effectively at zero temperature for $\varepsilon \gg 2$ μeV since then $\langle n\rangle \ll 1$. The emission current at higher temperatures follows from $I_{inel}(\varepsilon > 0, T) = e(\langle n\rangle + 1)A(\varepsilon)$, whereas the absorption current follows from $I_{inel}(\varepsilon < 0, T) = e\langle n\rangle A(-\varepsilon)$: The reconstructed current spectrum is shown in Fig. 2B. The central part of the curves ($|\varepsilon| < 10$ μeV) is kept blank because Eq. 1 does not include the T-dependence of I_{el}. The calculated current reproduces the measured current well up to 200 mK. Even the small step-like feature seen at ε » 30 μeV is reflected by a shoulder-like feature at ε » -30 μeV in the measured and in the calculated absorption spectra (indicated by arrows). For T > 200 mK, the measured current significantly exceeds the calculated current, which is probably due to thermally excited electrons (Eq. 1 only describes the T-dependence of the environment. The thermal excitations in the electron leads are not included.) Further confirmation of the applicability of the Einstein relations to our quantum dot system follows from the prediction: $[I_{inel}(\varepsilon > 0) - I_{inel}(\varepsilon < 0)]/eA(|\varepsilon|) = [W_e - W_a]/A = 1$, which is valid independent of T. Figure 2C shows a plot of the normalized rates, W_a/A and W_e/A, versus $kT/|\varepsilon|$ for various ε and T up to 200 mK. The measured data closely follow the prediction $[W_e - W_e]/A = 1$; that is, the normalized rates, W_a/A and W_e/A, differ by one over the temperature range T < 200 mK without fitting any parameter.

The inelastic rate for a two-level system coupled to a bosonic environment at T = 0 is expected to have a T_c^2 dependence (14, 15). Still without identifying the bosonic environment, we can test this dependence on the elastic tunnel coupling T_c between the two dots. Figure 3A shows that the inelastic current clearly increases with T_c. For the largest coupling, we obtain a saturation where the elastic current peak can no longer be distinguished. By fitting the elastic current part to a Lorentzian line shape (11) we can obtain rough estimates for T_c as long as the current is less than the saturation value. We find that with these fitted values, the inelastic current scales as T_c^{α} with an exponent $\alpha = 2.5$ » 3, maybe somewhat greater than expected. Figure 3B shows the effect of the increased coupling on the symmetric part of the current at low T. For small tunnel coupling, we always obtain Lorentzian line shapes. For increasing couplings, the data still fits to a Lorentzian tail on the absorption side. However, we generally find significant deviations for small ε, implying that for large coupling the elastic and inelastic rates can become of the same order. This effect may form a significant limitation for the coherence time in coupled quantum devices (16).

The importance of fluctuations in the environment on electron tunneling through quantum devices has been recognized for a long time. Environmental studies on Coulomb blockade devices with two- or more tunnel junctions have only discussed effects due to absorption (3, 17). For emission it is required that electrons are first pumped to a higher energy state, as has recently been done in a superconducting Cooper pair transistor under microwave irradiation (18). In the case of a double dot, pumping occurs when $E_L > E_R$ and an electron tunnels in from the left reservoir to E_L. A double dot thus offers

a unique two-level system that is pumped by a dc voltage without inducing heating currents. It is therefore possible to reach an out-of-equilibrium situation so close to T = 0 that vacuum °uctuations become the main source for generating electron transport.

To identify whether photons, plasmons, or phonons form the bosonic environment (19), we measured spontaneous emission spectra while placing the double dot in di®erent electromagnetic environments. In the regime from 10 to 100 ¹eV, the typical wavelengths are 1 to 10 cm for photons and 0.3 to 30 cm for 2DEG plasmons. We have tested the coupling to the photonic environment by placing the sample in microwave cavities of di®erent size (20). To check the coupling to plasmons, we have measured di®erent types of devices with largely di®erent dimensions of the 2DEG leads, gate pads, and bonding wires. Both types of variation had no e®ect at all on the emission spectra; even the ¯ne structure was reproduced.

The third option of acoustic phonons is the most likely possibility (21). Phonon emission rates have been calculated for single dots (22). For a double dot system, we can obtain the general energy dependence (15). For a deformation potential, we expect a rate dependence of $"^{D\,i\,2}$ (" for 3D phonons and constant for 2D phonons) and for piezo-electric interaction of $"^{D\,i\,4}$ (1=" for 3D phonons and $1="^2$ for 2D surface acoustic waves) (23). In Fig. 3C we compare traces measured on two di®erent types of devices. Here, the emission current is plotted versus " on a log-log scale. Ignoring the bumps, we ¯nd an energy dependence between 1=" and $1="^2$. This result implies that the dominant emission mechanism is the piezo-electric interaction with 2D or 3D acoustic phonons. Note that a 1=" or $1="^2$ dependence should be avoided in coherent devices, since the inelastic rate becomes large near resonance (" » 0) (16).

The bumps observed in both type of devices suggest the existence of resonances, for instance, due to a ¯nite size in the phonon environment. The bumps are particularly clear in the derivative of the current to energy (dotted curves in Fig. 3A). The large bump in Fig. 3A at " = 30 ¹eV corresponds to a frequency of f = "=h = 7.3 GHz. For 3D phonons this yields a wavelength $¸^{3D} = s^{3D}=f$ = 640 nm (s^{3D} = 4800 m/s is the 3D sound velocity), whereas for 2D surface acoustic waves $¸^{2D} = s^{2D}=f$ = 380 nm (s^{2D} = 2800 m/s). Both wavelengths, more or less, ¯t with the dimensions of the two quantum dot devices. We have not yet been able to control these resonances by studying devices with a variety of gate dimensions. However, we believe that it is possible to gain control over the phonon environment by making 3D phonon cavities in hanging bridges (24) or by creating a 2D phonon band gap with a periodic gate geometry (25).

[1] H. Mizuta and T. Tanoue, The Physics and Applications of Resonant Tunnelling Diodes (Cambridge Univ. Press, Cambrige, 1995).

[2] The New Superconducting Electronics, Proceedings of a NATO Advanced Study Institute, H. Weinstock and R.W. Ralston Eds. (Kluwer, Dordrecht, 1992), ser. E, vol. 251.

[3] Single Charge Tunneling, H. Grabert and M. H. Devoret, Eds., (Plenum, New York, 1992) Ser. B, vol. 294.

[4] P. L. McEuen, Nature, 393, 15 (1998); S. J. Tans, A. R. M. Verschueren, and C. Dekker, Nature, 393, 49 (1998).

[5] T. Fujisawa and S. Tarucha, Superlattices Microstruct. 21, 247 (1997); Jpn. J. Appl. Phys. 36, 4000 (1997).

[6] See for recent popular reviews: R. Ashoori, Nature 379, 413 (1996); L. P. Kouwenhoven and C. M. Marcus, Physics World, pp.35-39 (June 1998).

[7] For a review, see L. P. Kouwenhoven et al., in Mesocopic Electron Transport, Proceedings of a NATO Advanced Study Institute, L. L. Sohn, L. P. Kouwenhoven, and G. Schön, Eds., (Kluwer, Dordrecht, 1997), ser. E, vol. 345, pp. 105-214; available on line at http://vortex.tn.tudelft.nl/»leok/papers/.

[8] P. W. Milonni, The Quantum Vacuum, an Introduction to quantum electrodynamics (Academic Press, San Diego, 1994).

[9] The statistics of our inelastic emission should be regulated by the statistics of single-electron tunneling, see A. Imamoglu and Y. Yamamoto, Phys. Rev. B 46, 15982 (1992).

[10] The sample was cooled in a dilution refrigerator with a lowest temperature of 23 mK. Due to noise the e®ective electron temperature is »50 mK in the leads. In all measurements, we apply a perpendicular magnetic ¯eld between 1.6 and 2.4 T to maximize the single-particle spacing such that we can neglect transport through excited states.

[11] The elastic current is given by the formula $I_{elastic}(") = eT_c^2 ¡_R=[T_c^2(2 + ¡_R=¡_L) + ¡_R^2=4 + ("=h)^2]$, see Yu. V. Nazarov, Physica B 189, 57 (1993); T. H. Stoof and Yu. V. Nazarov, Phys. Rev. B 53, 1050 (1996).

[12] N. C. van der Vaart, et al., Phys. Rev. Lett. 74, 4702 (1995).

[13] Also co-tunneling can give excess current for " 6= 0. In our measurements, however, the co-tunneling current is less than 0.01 pA and can be neglected . For a review on co-tunneling see D. V. Averin and Yu. V. Nazarov, in Ref. 3, pp. 217-247.

[14] A. J. Legget, et al., Rev. Mod. Phys., 59, 1 (1987).

[15] A T_c^2-dependence can also be obtained from perturbation theory when T_c ¿ ", see L. I. Glazman and K. A. Matveev, Sov. Phys. JETP 67, 1276 (1988).

[16] We have reported a coherent coupling e®ect in double quantum dots using photon-assisted tunneling experiments, in T. H. Oosterkamp et al., Nature, in press. These observations are made when a small bias voltage is applied. In this case emission processes do not give rise to current.

[17] Stimulated emission into the electromagnetic environment does play an important role for having charging e®ects in single tunnel junctions. For instance, see: T. Holst et al, Phys. Rev. Lett, 73, 3455 (1994).

[18] Y. Nakamura, C. D. Chen, and J. S. Tsai, Phys. Rev.

Lett. 79, 2328 (1997).
[19] Bosonic excitations in a Fermi liquid (particle-hole excitations) can also be described as a bosonic bath with Ohmic dissipation. For this case, the inelastic rate has a power-law dependence, $¡(") » "^{°}$, where ° is related to the phase shift, ±, at the Fermi surface through: $° = 4=¼^2±^2 ¡ 1$ [See Ref. (14) and F. Guinea et al., Phys. Rev. B 32, 4410 (1985)]. Since $±^2 > 0$, the power $° > ¡1$. This does not agree with our observed energy dependence, which is between 1=" and $1="^2$.
[20] We used a cylindrical cavity (diameter = 36 mm and height = 84 mm) which has a minimum resonance energy of about 20 ¹eV, and a rectangular cavity (22 mm by 19 mm by 8 mm) with resonance frequency of about 40 ¹eV.
[21] Coupling to optical phonons is e±cient only at much larger energies.
[22] U. Bockelmann, Phys. Rev. B 50, 17271 (1994).
[23] For phonons the inelastic rate at T = 0 can be written as $¡_i » (T_c=")^2 J("=~)$ where $J(") » \frac{c^2(")}{"} g(")$ is the spectral function (14). The phonon density of states $g(") » "^{D}$ i 1, such that $¡_i » T_c^2 c^2(") "^{D}$ i 4. When we neglect possible ¯ne stucture in c("), we have for deformation potential c » " and thus $¡_i » "^{D}$ i 2, while for piezo-electric interaction c » constant and thus $¡_i » "^{D}$ i 4.
[24] A. N. Cleland and M. L. Roukes, Nature, 392, 160 (1998).
[25] J. M. Shilton, et al., J. Phys.: Cond. matter 8, L531 (1997).
[26] We thank M. Devoret, L. Glazman, S. Godijn, Y. Hirayama, J. Mooij, Yu. Nazarov, Y. Tohkura, N. Uesugi, M. Uilenreef, and N. van der Vaart for help and discussions. Supported by the Dutch Foundation for Fundamental Research on Matter (FOM), L.P.K. by the Royal Netherlands Academy of Arts and Sciences.

FIG. 1. (A) Double quantum dot device de¯ned in the 2DEG of a GaAs/AlGaAs hetero structure by focused ion beam implantation. The narrow channel connects the large 2D source and drain leads. Negative voltages (V_{GL}, V_{GC}, and V_{GR}) applied to the metal gates (G_L, G_C, and G_R; widths are 40 nm) induce three tunable tunnel barriers in the wire. The two quantum dots, L and R, respectively, contain »15 and »25 electrons; charging energies are »4 and »1 meV; and the measured average spacing between single-particle states are »0.5 and »0.25 meV. (B, C, and D) Energy diagrams (vertical axis) along the spatial axis through the dots (horizontal axis) for the tunnel situations: Absorption, elastic and emission. Thick vertical lines denote tunnel barriers. The continuous electron states in the leads are ¯lled up to the Fermi energies $¹_S$ and $¹_D$. The external voltage V_{sd} between leads opens a transport window of size: $eV_{sd} = ¹_S ¡ ¹_D$. The energy, $" ´ E_L ¡ E_R$, is de¯ned as the di®erence between the topmost ¯lled discrete-state of the left dot, E_L, and the lowest discrete-state for adding an extra electron to the right dot, E_R. (The interdot capacitance prevents that E_L and E_R are simultaneously occupied.) An elastic current can °ow when " = 0, otherwise a non-zero current requires absorption (" < 0) or emission of energy (" > 0). T_c is the tunnel coupling and $¡_i$ is the inelastic rate between the two dots. $¡_L$ and $¡_R$ are the tunnel rates across the left and the right barriers. (E) Typical measurement of the current (solid) versus " at 23 mK. The measured current is decomposed in an elastic (dashed) and an inelastic (dotted-dashed) part.

FIG. 2. (A) Measured current versus " for T = 23 to 300 mK. The current is measured for eV_{SD} = 140 ¹eV while sweeping V_{GR} and V_{GL} simultaneously in opposite directions such that we change the energy di®erence ". Gate voltage is translated to energy " by a calibration better than 10% using photon-assisted tunneling measurements (16). Dashed lines indicate exponential dependence, $e^{"=kT}$, for j"j À kT. Arrows point at step-like structure on the emission side (" > 0) and a shoulder on the absorption side (" < 0). >From ¯ts (11) to the elastic current part at 23 mK we obtain $h¡_R ¼ hT_c ¼ 1$ ¹eV and $h¡_L ¼ 5$ ¹eV for this dataset. (B) Reconstructed current, $I_{tot}(") = I_{el}(23mK) + I_{inel}(";T)$ for different T. The spontaneous emission spectrum derived from the measured data at 23 mK and Eqs. 1 are used to reconstruct the full temperature and energy dependence. (C) The absorption rate W_a (open symbols) and emission rate W_e (closed symbols) normalized by the spontaneous emission rate A versus kT=j"j. Circles, squares, upper- and lower-triangles, and diamonds are taken at j"j = 18, 24, 40, 60, and 80 ¹eV, respectively (see also symbols in A). The solid line indicates the Bose-Einstein distribution, hni, whereas the dashed line shows hni + 1.

FIG. 3. Current spectrum for di®erent coupling energies at 23 mK. (A) The magnetic ¯eld is 1.6 T for (i) and 2.4 T for the other curves (10). The curves have an o®set, and curve (i) is multiplied by 5. Rough estimates for the coupling energies are: (i) hT_c (» 0.1 ¹eV; h is Planck's constant) ¿ $h¡_R$ (» 10 ¹eV), (ii) hT_c ¼ $h¡_R$ (» 1 ¹eV), (iii) hT_c > $h¡_R$ (» 0.1 ¹eV), and (iv) hT_c À $h¡_R$ (» 0.01 ¹eV) and $¡_L$ & $¡_R$ for all curves. The two dotted curves are the derivatives $¡dI=d"$ in arbitrary units for curves (i) and (ii) to enhance the bump-structure. (B) Logarithmic-linear plots for (i) and (ii). Dashed lines are Lorentzian ¯ts. For (ii) we chose parameters that ¯t the tail for negative ". (C) Logarithmic-logarithmic plots of the emission spectrum for two di®erent samples. The sold lines are taken on the FIB sample in Fig. 1A (upper trace is the same as (ii) in A; lower trace is for coupling energies between (i) and (ii) in A). The dotted line is taken on a surface gate sample with a distance between left and right barriers of 600 nm (12). The dashed lines indicate a $1="$ and $1="^2$ dependence expected for piezo-electric interaction with 3D and 2D phonons, respectively.

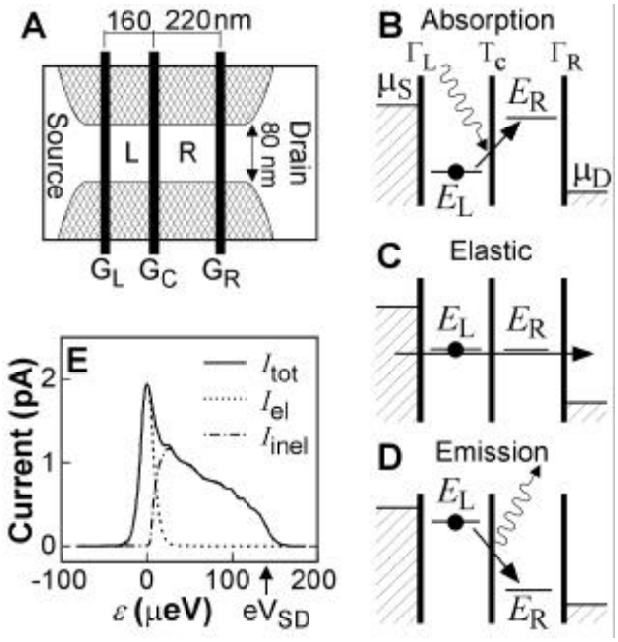

Fig. 1

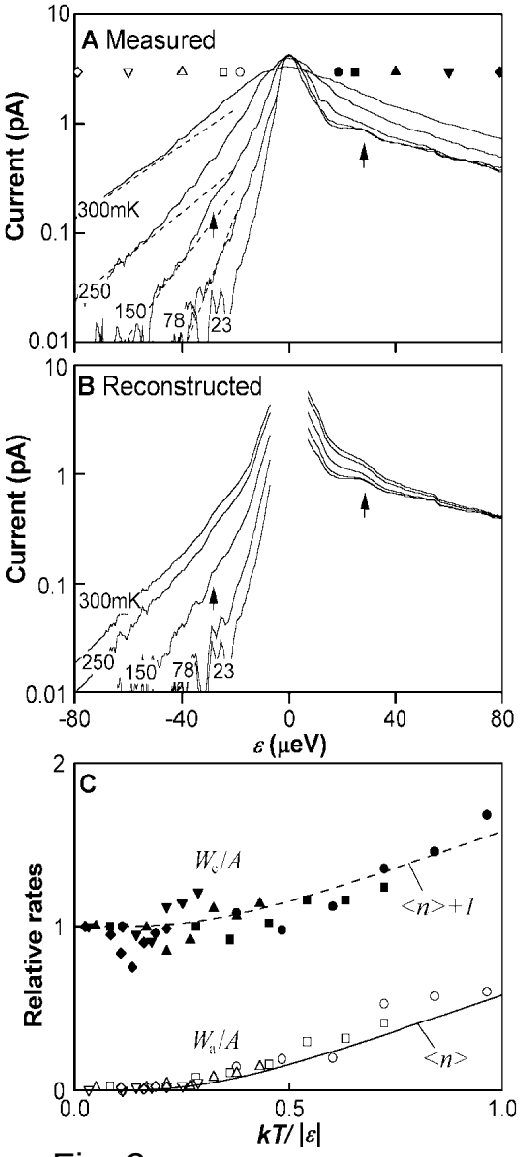

Fig. 2

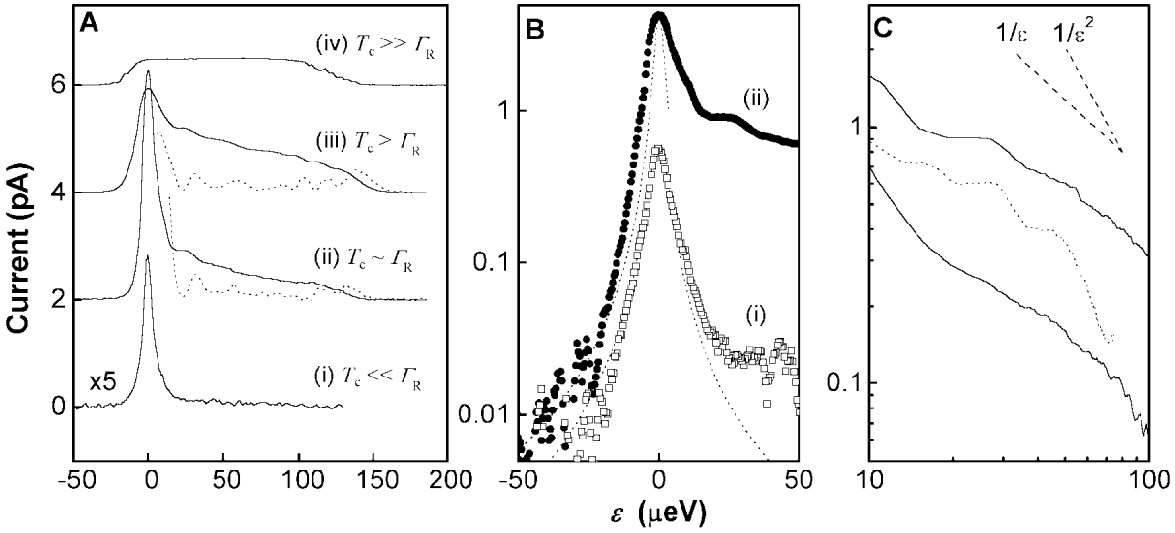

Fig. 3